This article is part of the

Proceedings of the 16th Minisymposium Verfahrenstechnik and 7th Partikelforum (TU Wien, Sept. 21/22, 2020)

Title:
Influences of Selective Waste Gas Recirculation on the Sinter Plant Process

Corresponding author:
Johannes Niel (TU Wien - ICEBE), johannes.niel@tuwien.ac.at

Date of submission:
23.07.20

Date of revision:
24.08.20

Date of acceptance:
27.08.20

Chapter ID:
MoV2-(02)

Length:
5 pages

Download available from (online, open-access):
http://www.chemical-engineering.at/minisymposium

ISBN (full book):
978-3-903337-01-5

Influences of Selective Waste Gas Recirculation on the Sinter Plant Process

Johannes Niel[1*], Bernd Weiß[2], Walter Wukovits[1]

1: TU Wien, Institute of Chemical, Environmental & Biological Engineering, Vienna, Austria
2: Primetals Technologies Austria GmbH, Linz, Austria
* Corresponding author: johannes.niel@tuwien.ac.at

Keywords: sinter plant model, selective waste gas recirculation, process simulation, distribution functions, SO_2 reduction, energy reduction

Abstract

Operating a sinter plant is material consuming and an energy intense process. It has vast impacts on the hot metal production and on the environment. Selective waste gas recirculation (SWGR) has been introduced to complement the sintering process to reduce energy consumption, waste gas volume and SO_2 emissions. Simulating this complex process is an attractive and low-cost opportunity for testing new operational settings.
The sinter plant implementation in gPROMS ModelBuilder® characterises the processes based on three sub-models. A burner model describes gas combustion, a black box model characterises the most important sinter strand processes and a wind box model splits the total off-gas stream into a recycle gas and a stack gas. A specific temperature polynomial was developed to represent the temperature distribution over the wind boxes enabling more detailed investigations of SWGR and a stable calculation of the sinter process in highly integrated flowsheets of iron production facilities.
Introducing SWGR to the sinter process, the model shows reduced coke consumption, stack gas and sulphur dioxide emissions by 11%, 27% and 27%, respectively. The sinter binding capacity of SO_2 has the highest influence on lowering SO_2 emissions under SWGR conditions.

Introduction

Using sinter has many positive aspects for the blast furnace process such as high porosity, stable mechanical properties, improved melting behaviour and constant chemical composition. Besides the agglomeration/melting process, carbon combustion, calcination, iron oxidation, vaporisation and liquification of water occur during iron ore sintering. Input properties and process conditions have vast influences on all reactions and on the final sinter product [1].
Solid input for the sinter process comprises iron carrier (e.g. iron ores), additives (e.g. limestone, dolomite, burned lime) and fuels (e.g. coke breeze, coal). The gaseous input includes air and gaseous fuels (e.g. natural gas, blast furnace gas) [1].
In the sinter process, first raw materials are mixed in a rotary drum. Water is added to achieve a homogeneous particle size through agglomeration at the granulator. In the next step, the raw mixture is put on moving pallet cars. Under the ignition hood, the sintering reaction is started on the top of the sinter

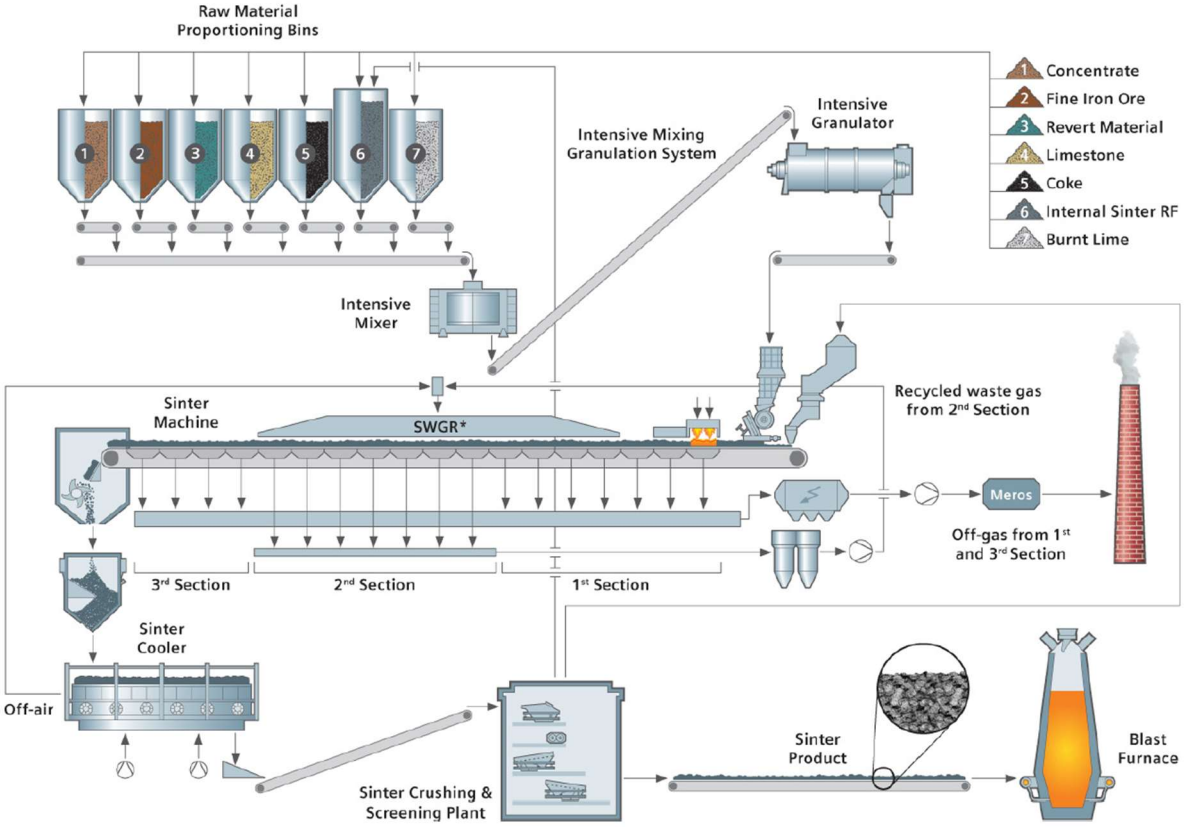

Figure 1: Schematic scheme of the sintering process [2]

bed. Gas is sucked through the sinter bed by blowers located under the sinter strand and the sintering reaction is moving to the bottom of the sinter bed. At the end of the sinter strand, produced sinter is crushed, cooled, and sieved into three fractions. The sinter fines, the first fraction, are recirculated to the proportioning bins, the second fraction is used as heart layer at the pallet cars, and the third fraction is the sintered product to be used in the blast furnace [3].
Underneath the sinter strand, wind boxes are collecting the entire gas stream, which varies over the total sinter strand length on its volume flow, composition and temperature. SWGR of single wind box gas flows to the sinter conveyor hood reduces fuel consumption, emissions and the off-gas volume [4]. Figure 1 shows a scheme of a general sintering process with SWGR.
The challenge of describing the general sintering process is its complexity, since every aspect of iron ore sintering is interconnected. To predict sinter plant behaviour accurately, a universal balancing model is an option to obtain useful information about the process and the plant design.
A flexible sinter plant model, which describes the effects of SWGR under different geometries, has the advantage of predicting operational conditions for various sinter plants. An appropriate calculation of temperature, composition and volume of the stack gas, the recirculated gas stream and the produced sinter is useful for sinter plant operators and engineers.

Sinter Model

The sinter plant model is developed in gPROMS ModelBuilder® (6.0.4, Process Systems Enterprise limited, December 2019) and characterises main process effects based on three sub-models. A burner model calculates the composition and properties of the combustion gas and the amount of combustion air under adiabatic conditions. A black box model describes the general sintering process, including main chemical reactions, gas-solid separation, mass and energy balances. A wind box model calculates gas flow and temperature of each wind box based on empirical distribution functions and splits the gas flow from the wind boxes into an off-gas and a recycle stream. *Figure 2* shows a schematic illustration of the sinter plant model.

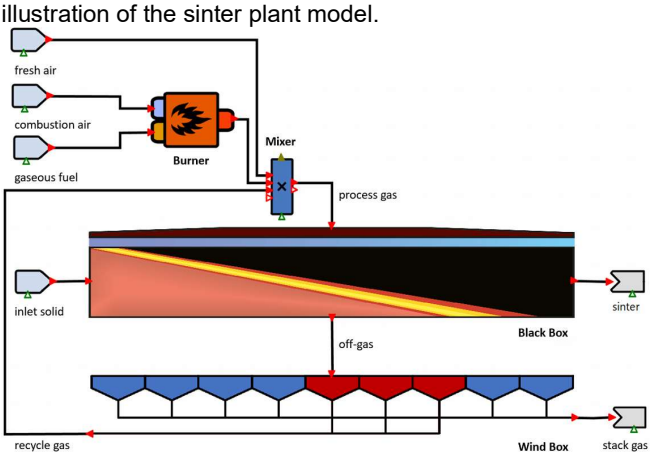

Figure 2: Sinter plant *model in gPROMS*

Burner Model

The fundamentals of the burner model are based on the assumptions in Beahr and Kabelac [5]. The air to fuel equivalence ratio λ defines the amount of combustion air (Eq.1). $\dot{m}_{air}$ is the mass flow of total air, $\dot{m}_{air,stoic}$ is the mass flow of air under stoichiometric conditions and $x_{O_2,air}$ and $x_{O_2,stoich}$ are the content of oxygen under real and stoichiometric conditions, respectively.
Equation 2 describes the chemical conversions of each gaseous fuel (CO, $C_xH_{y,(g)}$) with the reaction degree RD (Eq. 2). RD describes the stoichiometric conversion of each chemical reaction. $\dot{m}$ is the mass flow, x is the mass-based composition, RD is the reaction degree and MW is the molecular weight. The index k stands for the chemical component k, in for all input streams and out for the output stream. Based on the enthalpy balance (Eq. 3), the adiabatic flame temperature is calculated. Non-adiabatic conditions are considered by the enthalpy losses $\dot{H}_{losses}$. $h(T)$ is the specific enthalpy at temperature T.

$$\lambda = \frac{\dot{m}_{air} \cdot x_{O_2,air}}{\dot{m}_{air,stoich} \cdot x_{O_2,stoich}} \qquad \textit{Eq. 1}$$

$$\sum_{in}\left(\dot{m}_{in} \cdot \frac{x_{in,k}}{MW_k} \cdot RD\right) = \sum_{out}\left(\dot{m}_{out} \cdot \frac{x_{out,k}}{MW_k}\right) \qquad \textit{Eq. 2}$$

$$\sum_{in}\left(\dot{m}_{in} \cdot x_{in,k} \cdot h_k(T)\right) = \sum_{out}\left(\dot{m}_{out} \cdot x_{out,k} \cdot h_k(T)\right) + \dot{H}_{losses} \qquad \textit{Eq. 3}$$

Black Box Model

In the black box model the mass and enthalpy balance are applied along with stoichiometry of the sinter reactions (Eq. 2-3) [2]. Table 1 shows all chemical reactions of the black box model. It includes iron ore oxidations, main calcination reactions, carbon combustion, oxidations of sulphur and alkali and vaporization of water.
Following Schmid et. al. [6] increased sulphur binding in the sinter is observed in scenarios with SWGR. This behavior is considered in the model via the back reaction of SO_2 to S based on an empirical factor.
In difference to the burner model, additionally a gas and solid separation for the output streams is considered.

Table 1: Considered chemical reactions

C gasification	**water vaporisation**
$C + O_2 \rightarrow CO_2$ $C + ½\ O_2 \rightarrow CO$	$H_2O_{(l)} \rightarrow H_2O_{(g)}$ $Fe_2O_3{*}H_2O \rightarrow Fe_2O_3 + H_2O_{(g)}$
CO combustion	**chlorine**
$CO + ½\ O_2 \rightarrow CO_2$	$Cl + H \rightarrow HCl$
CO_2 release	**alkaline metal**
$MgCO_3 \rightarrow MgO + CO_2$ $CaCO_3 \rightarrow CaO + CO_2$ $FeCO_3 \rightarrow FeO + CO_2$	$2\ K + ½\ O_2 \rightarrow K_2O$ $2\ Na + ½\ O_2 \rightarrow Na_2O$
Fe oxidation	**sulphur**
$Fe + ½\ O_2 \rightarrow FeO$ $3\ Fe + 2\ O_2 \rightarrow Fe_3O_4$	$S_{(s)} + O_2 \rightarrow SO_2$ $SO_2 \rightarrow S_{(s)} + O_2$

Wind Box Model

Component Distribution

Based on published contents of chlorine and SO_2 over the wind boxes, functions describing the component distributions were implemented in the wind box model [7]. Each distribution is regressed based on dimensionless length (Eq. 5).

$$\frac{\dot{m}_j(x_i)}{\dot{m}_{j,total}} = \frac{a_j \cdot x_i^4 + b_j \cdot x_i^3 + c_j \cdot x_i^2 + d_j \cdot x_i + e_j}{\sum_i (a_j \cdot x_i^4 + b_j \cdot x_i^3 + c_j \cdot x_i^2 + d_j \cdot x_i + e_j)} \qquad \text{Eq. 5}$$

In Eq. 5, j is the index for components and i for the wind box number, a, b, c, d and e are the regression coefficients, x denotes for the dimensionless length of the wind box position and $\dot{m}_{j,total}$ is the total amount of component j. This equation design enables simulations for different plant geometries. Component and mass distribution can be used for a feed-forward and feed-backward oriented calculation. Figure 3 shows the implemented distribution functions.

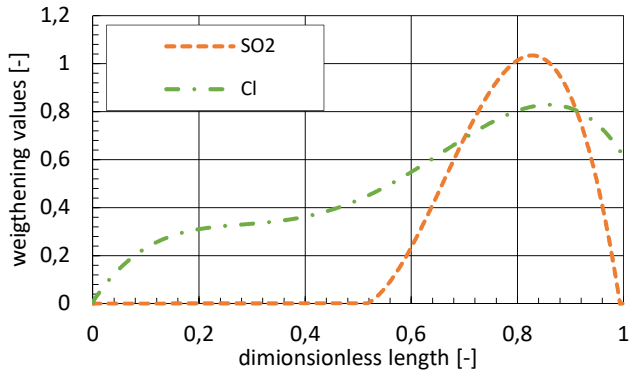

Figure 3: Implemented distribution functions

Temperature Distribution

Following Eq. 6, the temperature calculation of each wind box T(i) considers the off-gas temperature $T_{off\text{-}gas,BB}$ from the black box model ($T_{off\text{-}gas,BB}$= $T_{inlet,WB}$). $T_{inlet,WB}$ is multiplied with an explicit weighting term. This term includes the regressed function $T_{poly}(i)$, which takes into account the characteristic shape of the temperature distribution over the length of a sintering plant based on observed sensor data, and $T_{leveling}$, a fitting parameter, to ensure a closed enthalpy balance.

$$T(i) = T_{inlet,WB} \cdot \frac{T_{poly}(i)}{T_{leveling}} \qquad \text{Eq. 6}$$

A characteristic temperature profile of a sinter plant is shown in Figure 4. In this case $T_{inlet,WB}$ equals 150°C and the weighting term is shown on the second y axis.

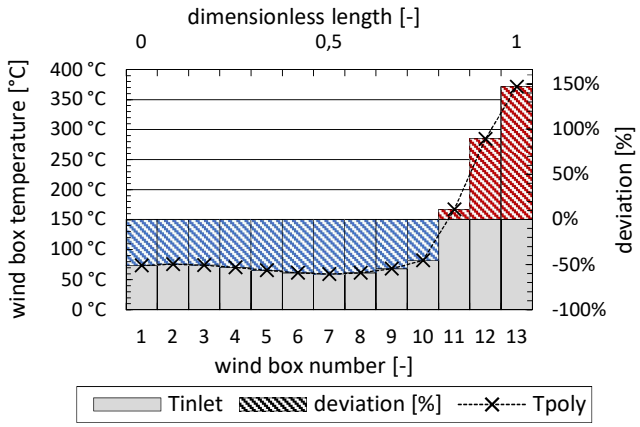

Figure 4: Wind box temperature distribution

Simulation Scenarios

The sinter plant model was applied to two scenarios: operation of the plant without SWGR and with SWGR. Both simulation scenarios had a mainly feed-forward oriented calculation structure. The number of wind boxes and the wind boxes used for waste gas recirculation were based on the publication by Schmid et. al. [7]. The gas flows of wind boxes 11 to 16 were recirculated at the SWGR scenario.

Both scenarios had the same sinter strand length, the same sinter production, the same ratio of total off-gas volume to produced sinter and the same conversion rates. Furthermore, the carbon monoxide and sulphur dioxide concentration of the stack gas flow as well as the temperature ratio of the last wind box to the sinter outlet were considered equal in both scenarios. The distribution functions of the wind box temperatures were based on plant data with and without SWGR. All input streams were kept constant; only one single coke stream was adjusted in the scenario without SWGR for ensuring comparable process temperatures in both scenarios. For the model validation plant data was provided by Primetals Technology GmbH and Voestalpine Stahl Linz GmbH.

Simulation Results

Measurements show that the average stack gas temperature at a sinter strand with SWGR is 21°C higher compared to a sinter strand without SWGR. The difference can be explained through different inlet temperatures of the process gas at both scenarios. As shown in Figure 5, the simulation results are in the range of measured plant data. Therefore, it is concluded, that the simulation scenarios represent realistic operational settings.

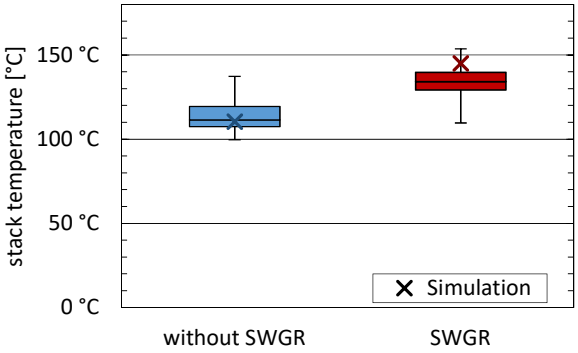

Figure 5: Stack temperature

Figure 6 shows all solid and liquid input and output streams of the sinter plant model. Corresponding to the scenario settings the sinter production is kept constant. As the simulation results show, this leads to the same input streams of iron carrier and additives in both scenarios. However, the resulting solid fuel and water streams are noticeable different.

In the SWGR scenario the coke consumption is reduced by 11% compared to the scenario without SWGR. This simulation result is in range with the observed effect on a real sinter plant (8-13%)[7][8].

There are two reasons for this effect:

(1) Through the recycle of carbon monoxide and its partly exothermic oxidization to carbon dioxide more heat is generated during the sintering process.

(2) By mixing fresh air and the recycle stream in the SWGR scenario, the process gas stream attained a higher temperature compared to the scenario without SWGR, which only uses fresh air. Therefore, less energy is necessary to enable the required process temperatures and, consequently, the coke amount declines.

An unexpected side effect is that more water needs to be added at the granulator to enable the same water ratio in the raw mixture in both scenarios, due to the natural water content of coke. Caused by the reduced coke input, the required water increases by 3.2% in the SWGR scenario compared to the scenario without SWGR.

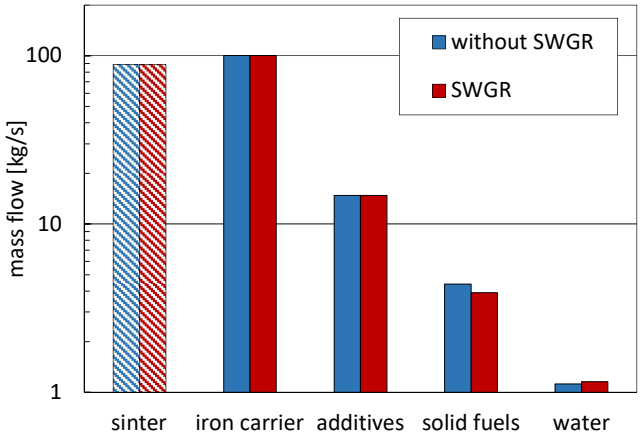

Figure 6: Comparison of solid input(plain) and output (hatched) streams

Figure 7 compares gaseous input and output streams based on the assumption of a constant ratio of total off-gas to produced sinter for the scenario with and without SWGR. In the scenario without SWGR, the amount of fresh air and process air are identical because no gas stream is recirculated from the wind boxes. In the scenario with SWGR, the fresh air consumption is decreased since process air contains the recirculated gas stream and fresh air.

Process air is the summation of fresh air, recycled gas and combustion gases from the ignition hood. The total process air consumption is similar in both scenarios. The slightly higher amount of total process air and off-gas in the scenario with SWGR can be explained with the constant ratio of total off-gas to produced sinter. In the SWGR scenario, more oxygen is bonded to carbon atoms by oxidising recirculated carbon monoxide. Therefore, slightly more fresh air is needed to obtain the same defined ratio at constant sinter production. In comparison, the lower coke amount remaining in the sinter and the reaction of sulphur dioxide to sulphur (sulphur binding in sinter) have lower influence on declining the amount of fresh air.

Due to the reduction of fresh air also the stack gas flow is lower in the scenario with SWGR.

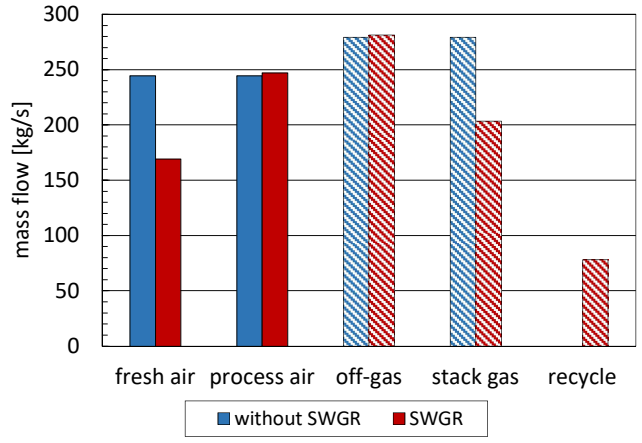

Figure 7: Comparison of gaseous input (plain) and output (hatched) streams

Figure 8 shows the change of total component flows of the SWGR scenario based on the scenario without SWGR in the stack gas. Introduction of SWGR effects each component flow in the off-gas stream differently.

The flow change of nitrogen correlates to the amounts of fresh air in both scenarios and decreases in the same ratio. In the SWGR case, the much lower oxygen flow can be explained by the reduction of fresh air and the further use of recycled O_2 for carbon and CO oxidations.

Surprisingly, the flow rate of CO_2 in the stack gas is slightly higher although the coke demand is reduced at the SWGR scenario. Both scenarios have similar production rates and produce the same amount of carbon dioxide during calcination. However, in the SWGR scenario, the entering carbon monoxide of the recycle is oxidized mainly to carbon dioxide, which explains the higher carbon dioxide flow in the SWGR scenario compared to the scenario without SWGR. Figure 9 shows this behaviour in more detail. The carbon monoxide and sulphur flows decrease at the same ratio as the stack gas since constant carbon monoxide and sulphur dioxide concentrations of the stack gas are assumed for the calculation following observations in the real sinter plant. In the SWGR scenario, the lower coke input stream has only a minor influence on the SO_2 reduction because the sulphur input mainly originates from iron and additive sources. The reduced sulphur content in the stack gas at unchanged sulphur inputs in the SWGR scenario is explained by higher sulphur binding in the sinter, considered by an empirical factor implemented in the simulation model. The nearly similar flows of water vapour in the stack gas is based on similar water inputs in the raw mixtures. The lower coke consumption in the SWGR scenario lowers the water content but the granulator compensates this effect by adding water in order to achieve the same water ratio in the raw mixture as in the scenario without SWGR.

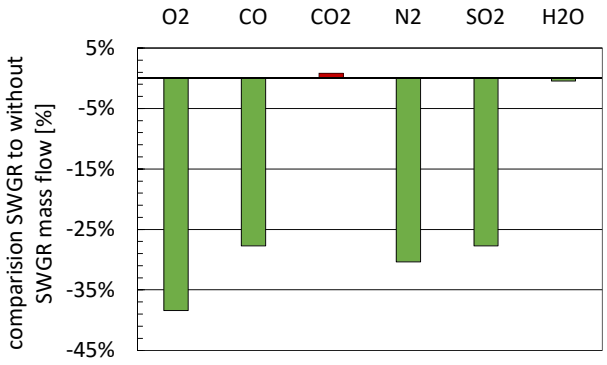

Figure 8: Comparison of main component flows in stack-gas

Figure 9 compares the CO_2 origin of both scenarios. In both cases, additives are the main carbon dioxide source and have a ratio of about two-third of the total carbon dioxide flow. The second largest CO_2 source originates from the coke combustion and the third and smallest CO_2 source arises from the CO oxidation. In contrast to the oxidation of recycled carbon monoxide, the declining coke consumption and its lower CO_2 oxidation has a minor influence on the CO_2 stream in the SWGR scenario. Therefore, the total carbon dioxide amount is higher compared to the scenario without SWGR as shown in Figure 8.

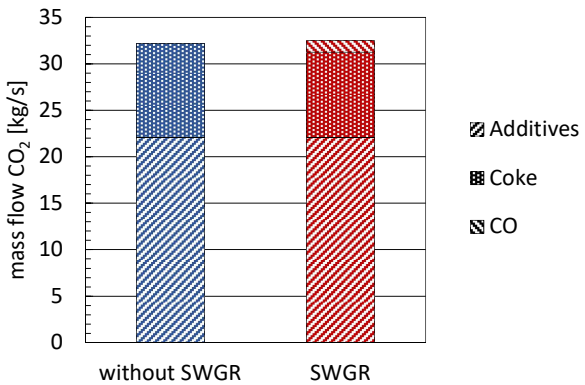

Figure 9: CO_2 origin

Figure 10 shows the mass flow of chlorine in the stack gas. About 85% of chlorine, which enters the sinter plant, is leaving the sinter plant via the stack. The given data show that the coke reduction has no significant influence on the chlorine amount in the stack gas.

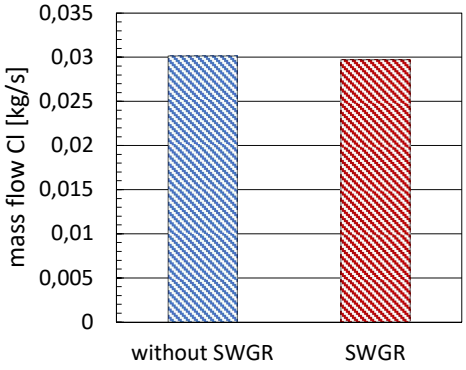

Figure 10: Chlorine content in stack gas

Most of the chlorine input originates form iron carrier input streams. Chlorine from coke and additive sources has a minor influence of around 10%. As shown in Figure 11, the changing coke consumption declines the total chlorine input amount by only 1%.

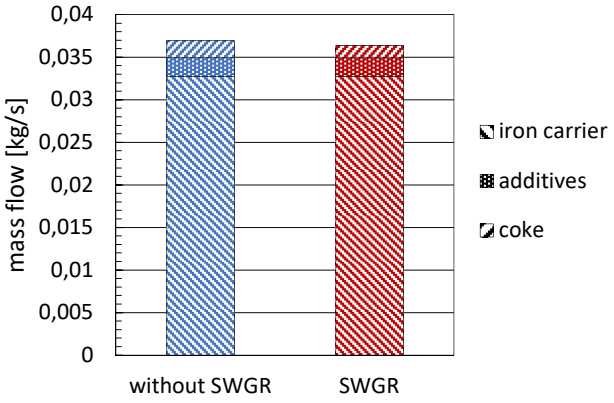

Figure 11: Origin of chlorine

Conclusion and Outlook

The comparison of the scenarios with and without SWGR shows that the sinter model gives reliable results compared to observed plant data. The simulated stack temperatures are in a proper temperature range. Under SWGR conditions, the model shows reasonable reduction of the coke demand, stack gas and SO_2 emissions by 11%, 27% and 27%.

In the SWGR scenario the total stack gas flow of CO_2 is higher compared to scenario without SWGR. This correlates to the oxidation of the recycled CO. The model considers the SO_2 binding capacity of sinter appropriately. In the SWGR scenario more sulphur is bound in the sinter and the SO_2 of the stack gas is reduced compared to the scenario without SWGR. The main sulphur sources are additives and iron carrier input streams. Under SWGR conditions, the sinter model shows only low reduction potential of chlorine emissions.

In the future, a correlation between the temperature function and the mass distribution function will be implemented in the model. It is expected that the model accuracy will be improved for changing plant geometries and operational settings. Additional investigations into trace element sources and reactions are recommended for improving the accuracy of the sinter model in a future detailed model.

Acknowledgement

The authors gratefully acknowledge the funding of work by the research program COMET (Competence Center for Excellent Technologies), the Austrian program for competence centers (FFG contract number 869295) and the support of Bernhard Rummer (Voestalpine Stahl Linz GmbH)and Herbert Schmid (Voestalpine Stahl Linz GmbH) in providing plant data and their expertise to this work.

References

[1] F. Cappel and H. Wendeborn, *Sintern von Eisenerze*. Düsseldorf: Stahleisen M.B.H., 1973.

[2] O. Almpanis-Lekkas, M. Mühlböck, B. Weiss, and W. Wukovits, “Model development of sinter plant with feasible selective waste gas recirculation,” vol. 11, no. 11, pp. 162–165, 2015.

[3] O. Almpanis-Lekkas, *Model development of metallurgical unit operations for use in a process simulation too*. Wien: Technische Univerität Wien, 2015.

[4] F. Cappel, *Wärmebehandlung des Sinters mit heißen Rauch- oder Prozeßgasen im Anschluß an den Zündofen*. Achen: RWTH Achen, 1977.

[5] H. D. Baehr and S. Kabelac, *Thermodynamik: Grundlagen und technische Anwendungen*. Berlin, Heidelberg: Springer Berlin Heidelberg, 2009.

[6] H. Schmid, W. Ehler, and E. Zwittag, *Operational Experience with the new eposint gas recycling process at sinter strand No 5 of voestalpine Stahl in Linz*, 2018.

[7] G. Brunnbauer, W. Ehler, E. Zwittag, H. Schmid, J. Reidetschläger, and K. Kainz, “Eposint- ein neues Konzept zur Abgasrückführung für Sinteranlagen,” *Stahl und Eisen*, vol. 126, no. 9, pp. 41–46, 2006.

[8] J. Reidetschläger, H. Stiasny, S. Hötzinger, C. Aichinger, and A. Fulgencio, “Siemens VAI sintering selective waste gas recirculation system: Meet the future’s environmental requirements today,” vol. 7, pp. 54–59, 2010.